http://dx.doi.org/10.5012/bkcs.2014.35.4.1023

Explaining the Drift Behavior of Caffeine and Glucosamine After Addition of Ethyl Lactate in the Buffer Gas of an Ion Mobility Spectrometer

Roberto Fernandez-Maestre,[*] Andres Reyes Velasco,[†] and Herbert H. Hill[‡]

Programa de Quimica, Campus de San Pablo, Grupo de Quimica y Medio Ambiente, Universidad de Cartagena, Cartagena, Colombia. [*]E-mail: rfernandezm@unicartagena.edu.co
[†]Departamento de Quimica, Universidad Nacional de Colombia, Bogota, Colombia
[‡]Washington State University, Department of Chemistry, Pullman, WA, 99164-4630, USA
Received November 4, 2013, Accepted December 5, 2013

Protonated caffeine (CH^+) and glucosamine (GH^+) overlapped in an analysis with ion mobility spectrometry-quadrupole mass spectrometry. Ethyl lactate vapor (L) at different concentrations from 0 to 22 mmol m^{-3} was added as a buffer gas modifier to separate these signals. The drift times of CH^+ and GH^+ increased with L concentration. The drift time increase was associated to clustering equilibria of CH^+ and GH^+ with one molecule of L and the equilibrium of GH^+ was more displaced to the formation of GLH^+ than that of CLH^+. GH^+ clustered more to L than CH^+ because GLH^+ formed more stable hydrogen bonds (26.30 kcal/mol) than CLH^+ (24.66 kcal/mol) and the positive charge in GH^+ was more sterically accessible than in CH^+. The aim of this work was to use theoretical calculations to guide the selection of a buffer gas modifier for IMS separations of two compounds that overlap in the mobility spectra and predict this separation, simplifying that empirical process.

Key Words : Dopants, Ethyl lactate glucosamine, Caffeine, Ion mobility spectrometry, Theoretical calculations

Introduction

Ion mobility spectrometry (IMS) is an analytical technique that separates gas-phase ions based on their size to charge ratios. Karasek (1970)[1] introduced IMS as a detector for volatile organic species and, nowadays, is a separation technique for the analysis of solid, liquid and gas-phase samples. IMS has been widely used in the pharmaceutical industry[2] especially for cleaning verification.[3] Tan and DeBono (2002) found IMS to be up to sixty times faster than HPLC for the cleaning verification in the pharmaceutical industry; they found IMS to be a versatile technique to identify and quantify a wide range of molecules, verify the cleaning process, and reduce the lead time of the drug development process.[4] Payne *et al.* (2005) obtained similar results and found that IMS complied with validation for precision, specificity, limits of detection and quantitation, accuracy, linearity, speed, and stability to determine residues of diphenhydramine on stainless steel surfaces.[5] Strege (2009) considered IMS attractive for at-line determination of residues on swabs taken from drug-manufacturing equipment for cleaning verification.[6]

The number of active ingredients in drugs and additives in food and the need for rapid qualitative separation and identification of these species are constantly increasing. The monitoring of diverse pharmaceutical products, that are manufactured using the same factory devices, is important to avoid cross-contamination of final products. Some of these compounds, such as caffeine and glucosamine, overlap in the mobility spectrum complicating their identification and quantification.

Modifiers such as 2-butanol[7] and ethyl lactate[8] added into the buffer gas of a mobility spectrometer cluster with overlapping analytes, selectively change their mobilities, and separate these analytes. When selected properly, modifiers can be used in this way to facilitate cleaning verification in pharmaceutical and food industries. However, the selection of the best modifiers to perform a separation is still a matter of trial and error and choices are empirical and based on chemical intuition.[7]

In this work, the drift behavior of a pair of drugs that partially overlapped in the IMS spectrum, caffeine and glucosamine, was investigated when ethyl lactate was introduced in the buffer gas. Theoretical calculations were performed to shed light on the origin of the differences in the mobility spectra upon addition of the modifier. Our study shows that theoretical calculations can be used to predict the possibility of a given separation in IMS by determining the strength of the drug-modifier interactions.

Experimental

Experimental conditions have been detailed elsewhere,[9] and a summary is given here. Experiments were performed using an ion mobility spectrometer at atmospheric pressure interfaced through a 40-μm pinhole to a quadrupole mass spectrometer and an electrospray ionization source (Figure 1).

Instrument. Parameters of operation of the mobility spectrometer were: voltage at the gate, 10.80 kV; gate clo-

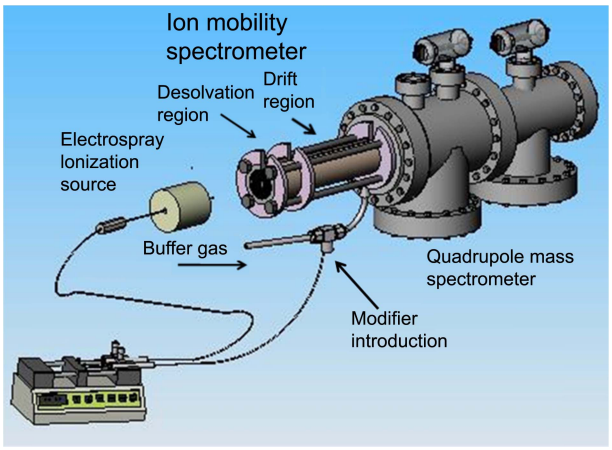

Figure 1. Ion mobility spectrometer coupled to a quadrupole mass spectrometer.

sure potential, ± 40 V; gate pulse width, 0.1 ms; scan time, 35 ms. The IMS had an electrospray ionization source and a 25 cm long drift tube. The tube had a desolvation region (7 cm) and a drift region (25 cm) separated by an ion gate. The drift tube was comprised of electric stainless-steel rings separated by insulating rings connected through resistors creating a 432 V cm^{-1} electric field in the tube.[10] N_2 buffer gas (0.9 liter min^{-1}; 150 ± 2 C) was injected countercurrent to the drift of ions by the end of the drift tube to desolvate the ions. The mobility instrument was run at 690-710 Torr, the atmospheric pressure in Pullman, WA, USA.

Modes of Operation. Ion mobility spectrometers coupled to quadrupole mass spectrometers produce spectra in three modes: single ion monitoring ion mobility spectrometry (SIM-IMS), radiofrequency-only ion mobility spectrometry (IMS), and mass spectrometry (MS). In SIM-IMS mode, the mass spectrometer voltages are set to detect only ions of a given mass or range of masses; SIM-IMS avoids the interference of other ions when determining a specific compound, and mobility spectra of a specific ion or ions are obtained. In IMS mode, the gate is pulsed continuously, the DC voltages in the mass spectrometer are turned off, and all ions reach the detector; the total IMS spectrum of the sample is obtained in this mode. In MS mode, all ions pass continuously, without pulsing, through the mobility spectrometer directly to the mass spectrometer, and are separated in the mass spectrometer; mass spectra are obtained in this mode.

Sample and Modifier Preparation and Introduction. Solutions of the analytes, caffeine and glucosamine (50-μM), were prepared in ESI solvent (47.5% methanol: 47.5% water: 5% acetic acid). Liquid samples or the solvent (ESI solution) were infused by electrospray ionization (voltage at the first ring, 12.12 kV). Ethyl lactate was continuously pumped into the buffer gas line at concentrations of up to 22 mmol m^{-3} before the buffer gas heater. To help vaporize ethyl lactate, a heating tape was wrapped around the buffer gas line.

Theoretical Study. Density functional theory calculations were performed employing the electronic hybrid exchange-correlation functional B3LYP and the electronic basis set 6-31G(d,p) with the GAMESS suite of programs.[11]

Results and Discussion

The Blank Solution Spectra in Pure Nitrogen Buffer Gas. Figure 2 shows the spectra of the electrospray solvent without introducing ethyl lactate in the buffer gas. IMS spectra were obtained in IMS mode. In this spectrum, the reactant ion peak was observed at 14.35 ms, corresponding to a reduced mobility of 2.49 $cm^2V^{-1}s^{-1}$. Figure 2(b) shows the mass spectrum of the solvent obtained in MS mode; this figure shows the main reactant ion peaks at *m/z* 19, H_3O^+, and the absence of contamination in the drift tube (only small peaks above *m/z* 19); a clean instrument is important because contaminants change the mobility of analyte ions by clustering.

The Blank Solution Spectra when Ethyl Lactate was Introduced in the Buffer Gas. Figure 3 shows the spectra of the electrospray solvent when 22 mmol m^{-3} of L was injected in the buffer gas; the IMS spectrum (Figure 3(a)) shows peaks at 26.88, L_nH^+ and $L_nH_3O^+$, and 27.80 ms, L_nNa^+; the peak at 26.88 ms, the clusters of reactant ions with L, showed a 87% drift time increase with respect to the peak at 14.35 ms in Figure 2, due to clustering equilibria with L:

$$H^+ + nL \Leftrightarrow L_nH^+$$

$$H_3O^+ + nL \Leftrightarrow L_nH_3O^+$$

$$Na^+ + nL \Leftrightarrow L_nNa^+$$

where n = 1, 2, or 3; the large increase in drift time is because small ions, such as the reactant ions, are more affected by clustering due to a large increase in their collision cross sections after attaching to a molecule. In the mass spectrum (Figure 3(b)), water and LX cluster peaks (where

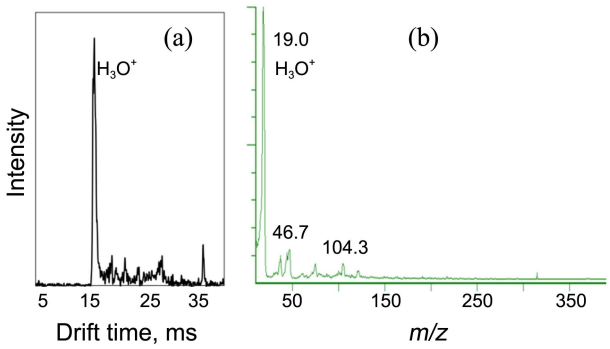

Figure 2. (a) IMS and (b) MS spectra of the electrospray solution (blank) in nitrogen buffer gas. (a) The main reactant ion peak, H_3O^+, appeared at 14.35 ms (2.49 cm^2 $V^{-1}s^{-1}$); (b) the peak at *m/z* 19 is H_3O^+. The clean MS and IMS spectra demonstrate absence of contamination in the instrument. The x axis is the drift time, the time the ions take to cross the drift region of the instrument.

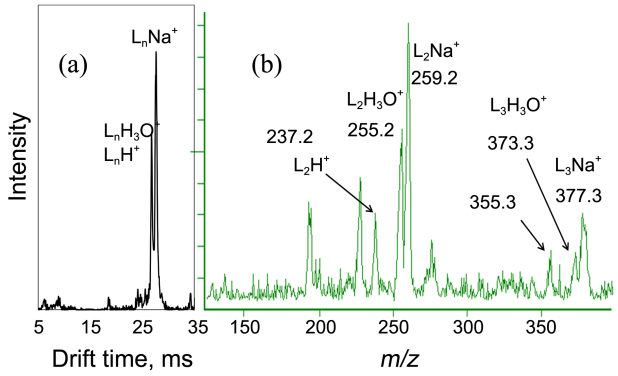

Figure 3. IMS (a) and MS spectra (b) of the electrospray solvent (reactant ions) when 22 mmol m^{-3} of ethyl lactate, L, were introduced into the buffer gas.

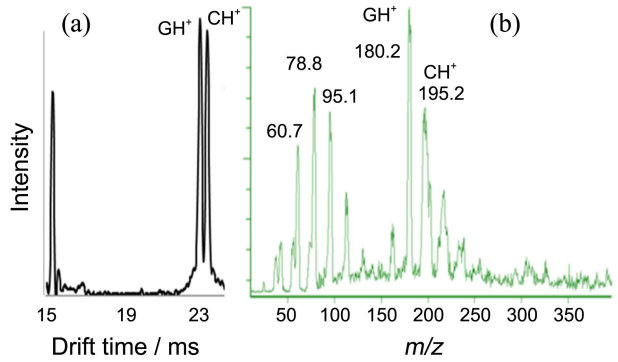

Figure 4. (a) Mobility and (b) mass spectra of a 50 μM mixture of caffeine and glucosamine in pure N_2 buffer gas; spectrum 4a shows the peaks of GH^+ and CH^+ partially overlapping at 23 ms; the peak at ~15 ms corresponds to the reactant ions peaks below *m/z* 100 in the mass spectrum b; spectrum b shows the MS peaks of CH^+ at *m/z* 195.2 and GH^+ at *m/z* 180.2.

X = H^+, H_3O^+, and Na^+) were absent below *m/z* ~190 due to clustering with the modifier indicating a saturation of the drift tube with ethyl lactate; clusters appeared at *m/z* 237.2 (L_2H^+), 255.2 ($L_2H_3O^+$), 259.2 (L_2Na^+), 355.3 (L_3H^+), 373.3 ($L_3H_3O^+$), and 377.3 (L_3Na^+).

Spectra of GH^+ and CH^+ in Pure Nitrogen Buffer Gas. Figure 4(a) shows the product ion peaks, GH^+ and CH^+, partially overlapping at 23 ms in the IMS spectrum of a solution of caffeine and glucosamine electrosprayed into the IMS with no modifier added to the buffer gas. Figure 4(b) shows the reactant ion peaks below *m/z* 100 and the MS peaks of GH^+ and CH^+ at *m/z* 180.2 and 195.2, respectively, for the same solution.

Behavior of GH^+ and CH^+ Upon Introduction of Ethyl Lactate in the Buffer Gas. Figure 5 depicts the drift behavior of GH^+ and CH^+ when L increased from 0 to 22 mmol m^{-3} in the buffer gas. In pure N_2 buffer gas, GH^+ and CH^+ partially overlapped with drift times of 22.75 ms and 23.10 ms, respectively; when the concentrations of L were 2.6, 5.1, 10, and 22 mmol/L the drift times of GH^+ and CH^+ increased to 23.07 and 23.17, 23.34 and 23.24, 23.62 and 23.37, and 24.32 and 23.83 ms, respectively: the

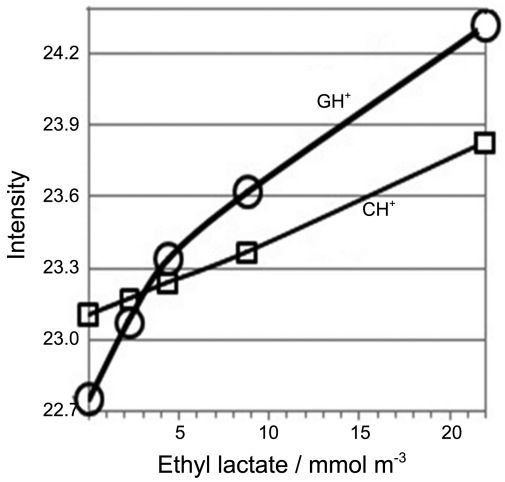

Figure 5. The drift times of CH^+ (□) and GH^+ (○) decreased when ethyl lactate, L, was introduced in the buffer gas of the mobility spectrometer.

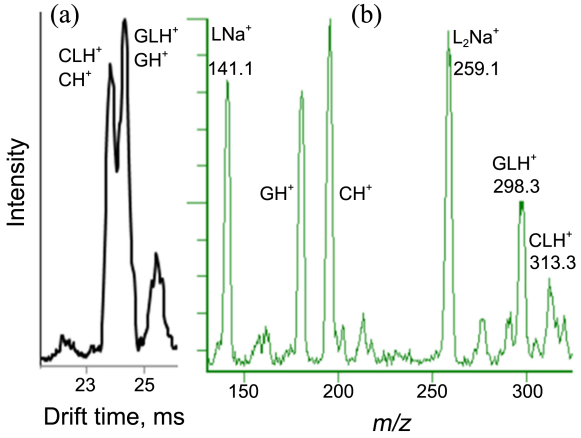

Figure 6. (a) Mobility and (b) mass spectra of the mixture of caffeine and glucosamine when 22 mmol m^{-3} of ethyl lactate were introduced into the buffer gas. The drift times of GH^+ and CH^+ increased with respect to Figure 4(a) due to formation of GLH^+ and CLH^+. No additional peaks between *m/z* 350 and 450 were found which indicated a negligible formation of clusters of GH^+ and CH^+ with two L molecules at these conditions.

positions of GH^+ and CH^+ swapped in the mobility spectrum. This increase in drift time was due to a selective formation of large CLH^+ and GLH^+ clusters as demonstrated in Figure 6.

Figure 6 shows the spectra of a mixture of caffeine and glucosamine when 22 mmol m^{-3} of ethyl lactate was introduced into the buffer gas at 150 °C; the MS spectrum in Figure 6(b) shows the peaks of GH^+, CH^+, GLH^+, and CLH^+ at *m/z* 180.2, 195.2, 298.3, and 313.3, respectively; the IMS spectrum in Figure 6(a) shows that the drift times of the peaks of GH^+ and CH^+ increased with respect to Figure 4(a) but to different extents; Figure 6(b) shows the absence of clusters of GLH_3O^+ and CLH_3O^+ which may indicate a high concentration of L in the buffer gas "sequestering" water and all ions; this sequestration would deter the equilibria of GH^+ and CH^+ with water because for these ions and molecule it

would be more probable to collide with ethyl lactate than with any other particle apart from nitrogen.

Three features in Figure 6 indicate that GH^+ clustered more with L than CH^+:

- The mass spectrum shows a GH^+ peak smaller than that of CH^+ while GH^+ is larger in Figure 4(b) (no modifier added); this indicates that the GH^+ peak decreased in favor of its cluster.
- The GLH^+ cluster peak is larger than that of CLH^+ (Figure 4(b)).
- GH^+ drifted slower than CH^+ which was the contrary to what is seen in Figure 4 (no modifier added).

The drift time increase depicted in Figure 5 between the drift times of GH^+ in pure nitrogen buffer gas and when 22 mmol m^{-3} of L were introduced in the drift tube corresponded to a mobility reduction of 7.1% (Table 1). Previous experiments with ethanolamine as analyte and L as the modifier have shown a mobility reduction of 41%, up to three ethanolamine-LH^+ clusters, and the absence of protonated ethanolamine when L was introduced into the buffer gas at concentrations of only 1.7 mmol m^{-3} (Table 1);[8] the smaller increase in drift time of GH^+ with respect to ethanolamine is because of the smaller size of the latter as explained in the text to Figure 3; the formation of only one cluster of GH^+ with L, GLH^+, in contrast to three for ethanolamine, is due to the larger accessibility to the charged amino group in ethanolamine than in GH^+. This open position in ethanolamine allowed for more extensive formation of clusters which depleted protonated ethanolamine; the low concentrations of L (1.7 mmol m^{-3}) required to show this extensive clustering support these explanations.

Drift Tube Equilibria. The reactant ions and their clusters appeared as a single peak in the IMS spectrum (Figure 3(a)) which indicates that they were in equilibrium in the drift tube. The same behavior was shown by sodium ion clusters with L. Similar equilibria was observed between CH^+ and CLH^+, and GH^+ and GLH^+. CH^+ had the same drift time of CLH^+ and GH^+ the same of GLH^+ (Figure 6(a)) as confirmed by SIM-IMS; this drift time equivalence indicates that GH^+ and CH^+ and their respective cluster ions crossed the drift tube together continuously switching between each other (but inside the quadrupole they were mass separated) as in the equilibria depicted in Figure 7.

The experimental data collected so far confirms there are equilibria of GH^+ and CH^+ with L which are responsible for the change in drift times of the analytes. The larger extent in the change in drift time of GH^+ over CH^+ indicates that its equilibrium with L is more inclined to the right hand side of equation (equilibria equations) than that of CH^+. This is a proof that GH+ presents more clustering with L than CH^+.

We propose that the larger increase in drift time of GH^+ with respect to CH^+ is because:

- GH^+ binds more strongly to L than CH^+
- There is a preferential formation of GLH^+ over CLH^+ because the binding sites of GH^+, the positive hydrogens in the primary amino group, are less sterically hindered to attachment of modifier molecules than the binding site of CH^+, the positive hydrogen in the secondary nitrogen of the five membered ring.

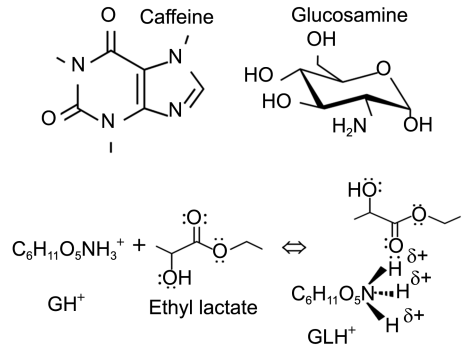

Figure 7. Structures of caffeine and glucosamine and equilibria between GH^+ and GLH^+.

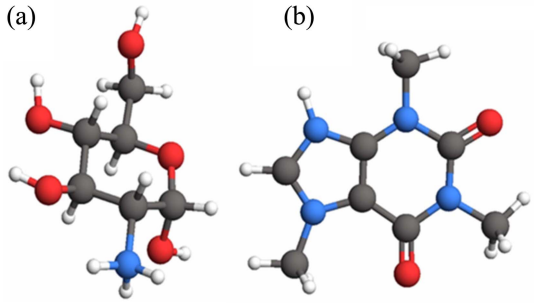

Figure 8. Optimized structures of protonated (a) Glucosamine and (b) Caffeine. Calculations were performed at the B3LYP/6-31G(d,p) level of theory.

Theoretical calculations have been performed to confirm the above hypotheses regarding the observed differences in clustering extents of GH^+ and CH^+.

Computational Study. Theoretical calculations were carried out at the B3LYP/6-31G(d,p) level of theory with the GAMESS suite of programs. Geometry optimization calculations were performed for ethyl lactate (L), caffeine (C) and glucosamine (G). The structures of C and G were later used as starting points to determine the geometries and energies of the protonated counterparts. Our calculations revealed

Table 1. Total energies of L, CH^+, GH^+, GLH^+ and CLH^+ and hydrogen bond energies calculated at the B3LYP/6-31G(d,p) level of theory with GAMESS.[11] GLH^+ formed more stable hydrogen bonds (26.30 kcal/mol) than CLH^+ (24.66 kcal/mol) which explains why GH^+ clustered more to L than CH^+

Species	Energy (hartree)	Hydrogen bond energies, kcal/mol
L	−422.01274	
CH^+	−680.37614	
GH^+	−667.34065	
CLH^+	−1,102.42817	−24.66
GLH^+	−1,089.39530	−26.30

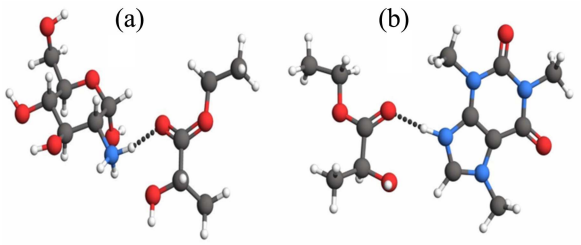

Figure 9. Optimized structures of the most stable hydrogen bond patterns of (a) GLH^+ and (b) CLH^+. Calculations were performed at the B3LYP/6-31G(d,p) level of theory.

that protons bind more strongly to G on the amino group and to C on the secondary nitrogen atom in the five membered ring. As shown in Figure 8, the protonated site of GH^+ is more easily accessible than that of CH^+ for the formation of hydrogen bonds with L.

Once GH^+ and CH^+ are formed in the electrospray source, they cluster with L in the drift tube. These clusters are bound by hydrogen bonds between GH^+ and CH^+ and one of the three hydrogen bond acceptor sites of ethyl lactate: the oxygen atoms of the carbonyl group, the hydroxy group, or the ether atom. Further calculations considering different hydrogen bond conformations of GH^+ and CH^+ and L were performed. As shown in Figure 9, the most energetically stable patterns were those in which the protonated moiety of GH^+ and CH^+ interacted *via* a hydrogen bond with the oxygen of the carbonyl group of L.

Hydrogen bond energies (E_{HB}) were estimated using $E_{HB} = E_{cluster} - E_L - E_{protonated\ analyte}$ and the energy data for CH^+, GH^+, GLH^+, and CLH^+ is shown in Table 1. We found E_{HB} of 26.30 kcal/mol and 24.66 kcal/mol for GLH^+ and CLH^+, respectively, which are in the range reported for hydrogen bond energies (−15 to −40 kcal/mol) for charged complexes.[12] These results show that L forms stronger hydrogen bonds with GH^+ than with CH^+ which explains the change in drift times for these ions.

Our computational calculations supported the hypotheses made to explain the larger increase in drift time of GH^+ with respect to CH^+ when ethyl lactate was injected in the buffer gas for which theoretical analysis may be useful to select the modifier for a given IMS separation.

Conclusions

IMS-quadrupole mass spectrometry with ethyl lactate vapor added to the buffer gas was used to try the separation of analytes that overlapped in a mobility spectrometer and theoretical calculations were performed to explain the observed drift behavior: GH^+ and CH^+ partially overlapped in the mobility spectrum using pure N_2 buffer gas; the drift time separation between GH^+ and CH^+ increased when ethyl lactate was vaporized in the buffer gas because GH^+ mobility decreased more than that of CH^+; this mobility decrease was due to formation of ethyl lactate clusters with GH^+ and CH^+.

We showed experimentally that GH^+ clustered more to ethyl lactate than CH^+ when this modifier was introduced in the buffer gas. Theoretical calculations showed that this preferential clustering of GH^+ was due to the fact that GLH^+ bound more strongly than CLH^+ and to the more open position of the positive charge in GH^+ than in CH^+ which allowed more interaction of GH^+ with ethyl lactate. These calculations also showed that the interactive group in ethyl lactate was the carbonyl group instead of the hydroxyl group as was considered before.[8]

A possible caveat of using modifiers to separate overlapping peaks is peak broadening due to clustering which may imply the requirement of large concentrations of modifier to separate the compounds. Despite this caveat, the method has been effectively used in the separation of overlapping compounds in IMS.[9]

Choosing a suitable modifier to separate overlapping ions in IMS is a question of trial and error. Theoretical calculations confirmed our hypotheses and explained our experimental results. We propose that theoretical calculations can be used as a tool to predict the best modifier to separate peaks that overlap in IMS. The energy difference of the ion-modifier bonds of a pair of ion-modifier clusters that allows a baseline separation of the overlapping peaks of these clusters must be determined to guide the selection of the modifier.

Acknowledgments. Dairo Meza, Universidad de Cartagena and Jorge Charry, Universidad Nacional de Colombia. And the publication cost of this paper was supported by the Korean Chemical Society.

References

1. Cohen, M. J.; Karasek, F. W. *J. Chromatogr. Sci.* **1970**, *8*, 330.
2. O'Donnell, R. M.; Sun, X.; Harrington, P. B. *Trends Anal. Chem.* **2008**, *27*, 44.
3. Strege, M. A.; Kozerski, J.; Juarbe, N.; Mahoney, P. *Anal. Chem.* **2008**, *80*, 3040.
4. Tan, Y.; DeBono, R. Today's Chemist at Work, November, 2004; p 15.
5. Payne, K.; Fawber, W.; Faria, J.; Buaron, J.; DeBono, R.; Mahmood, A. *Spectrosc. Mag. Online.* **2005**, January (Special issue) p 24, http://www.spectroscopyonline.com/spectroscopy/data/articlestandard/ spectroscopy/032005/143241/article.pdf.
6. Strege, M. A. *Anal. Chem.* **2009**, *81*, 4576.
7. Fernandez-Maestre, R.; Wu, C.; Hill, H. H. *Int. J. Mass Spectrom.* **2010**, *298*, 2.
8. Fernandez-Maestre, R.; Wu, C.; Hill, H. H. *Rapid Commun. Mass Spectrom.* **2012**, *26*, 1.
9. Fernandez-Maestre, R.; Wu, C.; Hill, H. H. *Curr. Anal. Chem.* **2013**, *9*, 485.
10. Wu, C.; Siems, W. F.; Asbury, G. R.; Hill, H. H. *Anal. Chem.* **1998**, *70*, 4929.
11. Schmidt, M. W.; Baldridge, K. K.; Boatz, J. A.; Elbert, S. T.; Gordon, M. S.; Jensen, J. J.; Koseki, S.; Matsunaga, N.; Nguyen, K. A.; Su, S. J.; Windus, T. L.; Dupuis, M.; Montgomery, J. A.; Adamovic, I.; Aikens, C.; Alexeev, Y.; Arora, P.; Bell, R.; Bandyopadhyay, P.; Bode, B.; Chaban, G.; Chen, W.; Choi, C. H.; Day, P.; Dudley, T.; Fedorov, D.; Fletcher, G.; Freitag, M.;

Glaesemann, K.; Merrill, G.; Netzloff, H.; Njegic, B.; Olson, R.; Pak, M.; Shoemaker, J.; Song, J.; Taketsugu, T.; Webb, S. GAMESS User's Guide, Iowa State University, 2007.

12. Desiraju, G. R.; Steiner, T. *The Weak Hydrogen Bond: In Structural Chemistry and Biology*; Oxford University Press: Weinheim, Germany, 2001; p 40.